Emerging Contaminants 5 (2019) 53–60

Contents lists available at ScienceDirect

Emerging Contaminants

journal homepage: http://www.keaipublishing.com/en/journals/emerging-contaminants/

Degradation of 2,4-dichlorophenoxyacetic acid by UV 253.7 and UV-H_2O_2: Reaction kinetics and effects of interfering substances

Asok Adak [a,*], Indrasis Das [b], Bijoli Mondal [a], Suman Koner [c], Pallab Datta [d], Lee Blaney [e]

[a] Department of Civil Engineering, Indian Institute of Engineering Science and Technology Shibpur, Howrah, 711103, India
[b] Department of Civil Engineering, Indian Institute of Technology Kharagpur, Kharagpur, 721302, India
[c] Department of Civil Engineering, Jalpaiguri Government Engineering College, Jalpaiguri, 735102, India
[d] Center for Healthcare Science and Technology, Indian Institute of Engineering Science and Technology Shibpur, Howrah, 711103, India
[e] Department of Chemical, Biochemical and Environmental Engineering, University of Maryland Baltimore County, USA

ARTICLE INFO

Article history:
Received 28 October 2018
Received in revised form
13 January 2019
Accepted 10 February 2019

Keywords:
2,4-D
UV-253.7
UV-H_2O_2
Advanced oxidation
Hydroxyl radicals

ABSTRACT

This work investigates the degradation of 2,4-dichlorophenoxy acetic acid (2,4-D) using UV irradiation and the UV-H_2O_2 advanced oxidation process (AOP). For UV irradiation at 253.7 nm, ~66% degradation was observed for a fluence of 20 J cm^{-2} and the apparent fluence-based, pseudo-first-order rate constant for 2,4-D was 5.77 ($\pm$0.66) $\times$ 10^{-5} cm^2 mJ^{-1}. With the UV-H_2O_2 AOP, approximately 97% degradation was observed for a fluence of 700 mJ cm^{-2}. Due to production of hydroxyl radicals, the apparent fluence-based rate constant was 100 times higher than that for direct UV photolysis. The effects of H_2O_2 dose, initial 2,4-D concentration, and water quality parameters, including pH (4–8), alkalinity (0–5 mM HCO_3^-), nitrate concentration (0–1 mM as NO_3^-), and ionic strength (0–17 mM as NaCl), were studied. The observed rate constants were dependent on pH, alkalinity, and nitrate concentration. The degradation of 2,4-D by the UV-H_2O_2 system was also examined in a real surface water. The observed fluence-based rate constant in the surface water matrix was 2.6 ($\pm$0.3) $\times$ 10^{-3} cm^2 mJ^{-1}, and this value was similar to a distilled water matrix containing the same alkalinity and pH. In addition, the biodegradability of UV and UV-H_2O_2 treated wastewater increased with irradiation time, suggesting that transformation products can be degraded by biological processes. Based on this study, the UV-H_2O_2 process represents a viable treatment method to transform 2,4-D into benign products.

1. Introduction

In the past few decades, agrochemicals (*e.g.*, pesticides and herbicides) have been widely used in intensive agriculture, a practice which has significantly contributed to increased contamination of surface water and groundwater supplies [1]. Pesticide pollution occurs from runoff from agricultural fields and equipment washing/rinsing practices [2]. Pesticide concentrations in wastewater from the agricultural and manufacturing industries have been reported to be 10–100 mg L^{-1} and 1–1000 mg L^{-1}, respectively, in different countries [1]. A number of reports have documented pesticide residues in groundwater, river water, lake water, drinking water, soil, and sediment in India [3,4]. Every freshwater body (*i.e.*, rivers, lakes, and estuaries) in India is expected to be contaminated with pesticides [5], and pesticide residues have been detected in cultivated vegetables [6].

Pesticides are classified depending on their usage: herbicides; insecticides; fungicides; rodenticides; nematicides; microbiocides; and, plant/insect growth regulators [7]. One of the most widely used herbicides in the world is 2,4-dichlorophenoxyacetic acid (2,4-D). In particular, 2,4-D is used for plant growth regulation and weed control; furthermore, 2,4-D is moderately toxic and potentially carcinogenic. Exposure to chronic oral doses has resulted in adverse effects on the eyes, thyroid, kidneys, adrenal glands, and ovaries [8]. Several literature reports show that 2,4-D negatively affects aquatic life, disturbs the ecosystem, and persists in the environment due to low biodegradability [9].

Due to the widespread presence of toxic pesticide residues in water resources, more efforts are required to remove these compounds from contaminated water. Adsorption onto activated

* Corresponding author.
E-mail address: asok@civil.iiests.ac.in (A. Adak).
Peer review under responsibility of KeAi Communications Co., Ltd.

https://doi.org/10.1016/j.emcon.2019.02.004

carbon is the most conventional and frequently employed treatment option for herbicides and pesticides [10,11]. Significant effort has gone into development of other sorbents like iron oxide-coated graphene oxide, surfactant-modified silica gel, chitosan beads, and silver-modified zero-valent iron nanoparticles for removal of pesticides from contaminated water [9,12–14]. Waste materials from the fertilizer and steel industries adsorbed 50% of 2,4-D for 15–30 min contact times and achieved up to 90% removal at equilibrium [15]. While adsorption processes have demonstrated an ability to remove pesticides from the aquatic environment, exhausted adsorbents can serve as a source of 2,4-D contamination, especially in areas without hazardous waste management facilities.

Coagulation-flocculation processes have been investigated for removal of 2,4-D [16]; however, low removal efficiencies of 40–50% were observed. Furthermore, disposal of the 2,4-D-laden water treatment residuals may present challenges for the reasons described above. Reverse osmosis systems demonstrate 70–90% removal of herbicides like atrazine, simazine, and diuron, but high energy costs and disposal of the herbicide-contaminated concentrate may be prohibitive in many areas [17]. Biodegradation of 2,4-D has been studied with *Pseudomonas* spp., *Achromobacter* spp., *Flavobacterium* spp., *Nocardia* spp., *Streptomyces* spp., and *Aspergillus* spp. [18]; however, the chlorine atoms in 2,4-D render this molecule resistant to biodegradation and increase environmental persistence [19].

In recent years, advanced oxidation processes (AOPs), including gamma irradiation in the presence of H_2O_2 [20], Fenton reactions [1], ozonation and catalytic ozonation [7,21], and ultrasonic and electrochemical oxidation [22], have demonstrated successful transformation of recalcitrant compounds like 2,4-D. Shu et al. reported second-order rate constants for micropollutant reaction with hydroxyl radicals and the electrical energy per order of transformation for various micropollutants, including 2,4-D, using a medium-pressure UV-H_2O_2 system [23]. UV-based AOPs have been studied for treatment of municipal and industrial wastewater containing recalcitrant organic contaminants, such as atrazine, 1,2-dibromo-3-chloropropane, and various pharmaceuticals [24–26]. In isolation, UV irradiation provides slow transformation for many organic molecules [27]. When hydrogen peroxide absorbs UV light, it undergoes rapid decomposition to form hydroxyl radicals [26]. Generally, low-pressure UV lamps that emit light at 253.7 nm are used for disinfection in water and wastewater treatment. At 253.7 nm, the hydroxyl radical yield is 1 mol of $HO^{\bullet}$ per mol of H_2O_2 [28]. Since hydroxyl radicals are highly reactive with organic molecules, the UV-H_2O_2 process is expected to effectively degrade 2,4-D. Nevertheless, many aspects related to the application of AOP treatment have not yet been explored for 2,4-D.

The objective of this study was to evaluate the effectiveness of 2,4-D treatment in agricultural wastewater by UV irradiation at 253.7 nm and the UV-H_2O_2 AOP. The specific aims of this study were as follows: (1) to map the molar absorption coefficients of 2,4-D as a function of pH and wavelength; (2) to determine the fluence-based reaction rate constants for UV and UV-H_2O_2 degradation of 2,4-D; and, (3) to identify the effects of water quality parameters, namely pH, alkalinity, nitrate concentration, and a real surface water matrix, on 2,4-D degradation. The overall goal of the work was to degrade 2,4-D to the point where biological processes can handle the transformation products.

2. Experimental materials and methods

2.1. Materials

Technical grade 2,4-D (98% purity; Sigma Aldrich, USA) and 30% H_2O_2 (Sigma Aldrich, USA) were used to generate synthetic wastewater and produce hydroxyl radicals (upon irradiation), respectively. Reagent grade $NaHCO_3$, H_3PO_4, NaH_2PO_4, Na,HPO_4, $NaNO_3$, and NaCl from Merck (India) were used to investigate potential interfering effects of pH, alkalinity, nitrate concentration, and ionic strength on the UV-H_2O_2 advanced oxidation kinetics for 2,4-D.

2.2. UV reactor

Direct photolysis and advanced oxidation reaction kinetics were studied using a batch UV reactor system that emitted monochromatic light at 253.7 nm (M/s. Lab Tree; Ambala, Haryana, India). The reactor was comprised of eight UV bulbs inside a metal enclosure with a highly polished stainless-steel reflector (see photograph in Fig. S1 of the Supplementary Information). Using ferrioxalate actinometry [29], the photon flux and fluence of the UV reactor were determined to be 1.9 ($\pm$0.1) $\times 10^{-4}$ E L^{-1} min^{-1} and 113 ($\pm$5.7) mJ cm^{-2} min^{-1}, respectively.

2.3. Experimental methods

A Thermo Fisher Scientific UHPLC system (Dionex Ultimate 3000) was used to measure 2,4-D. The analyte was separated on a C18 (4.6 $\times$ 250 mm, 5 μm) column at 35 °C. Acetonitrile (55%), 2% acetic acid (5%), and water (40%) from Merck (India) were used as the mobile phase. The flow rate and injection volume were 1 mL min^{-1} and 50 μL, respectively. The wavelength of the photodiode array (PDA) detector was set to 230 nm.

The molar absorption coefficients of 2,4-D were mapped across a pH range of 1–8 at wavelengths of 220–300 nm using a UV–visible spectrophotometer (Model 117, Systronics India Ltd.; Ahmedabad, India). Solution pH was maintained using 10 mM phosphate buffer and measured using a digital pH meter (PB-11; Sartorious GmbH). The apparent molar absorption coefficients of 2,4-D were attributed to the additive sum of contributions from the protonated and deprotonated species [21], as indicated by Eq (1).

$$\varepsilon_{app,\lambda} = \alpha_0\, \varepsilon_{0,\lambda} + \alpha_1\, \varepsilon_{1,\lambda} \quad (1)$$

In Eq. (1), $\varepsilon_{app,\lambda}$ is the apparent molar absorption coefficient at wavelength λ, α_i is fraction of species i at a particular pH, $\varepsilon_{i,\lambda}$ is the molar absorption coefficient of species i at wavelength λ, and the 0 and 1 subscripts refer to the protonated and deprotonated species (shown in Fig. 1), respectively.

All transformation experiments were conducted at 25 ($\pm$2) °C with 100 mL of wastewater that initially contained 100 mg L^{-1} of 2,4-D (0.45 mM). Similar concentrations have been reported to occur in agricultural wastewater, reinforcing the relevance of the experimental conditions [1]. Samples were irradiated for 6 h in a quartz beaker with covered upper and lower surfaces. Every 30 min, 1-mL aliquots were collected for 2,4-D analysis. The pseudo-first-order reaction kinetics for direct photolysis of 2,4-D in the batch reactor can be described by Eq. (2).

$$\ln\frac{C}{C_0} = -k'_{app}\, H' \quad (2)$$

In Eq. (2), C is the 2,4-D molar concentration at time t, C_0 is the initial 2,4-D molar concentration, k'_{app} is the apparent fluence-based, pseudo-first-order reaction rate constant (cm^2 mJ^{-1}), and H' is the fluence corresponding to time t (mJ cm^{-2}).

For advanced oxidation experiments, different H_2O_2 doses were investigated to identify the conditions that provide the fastest transformation kinetics. The following molar ratios of applied H_2O_2 to initial 2,4-D were tested: 0.5; 1.0; 2.5; 5.0; 7.5; and, 10.0. The pH of these solutions was approximately 4.0 ($\pm$0.1) due to the weakly

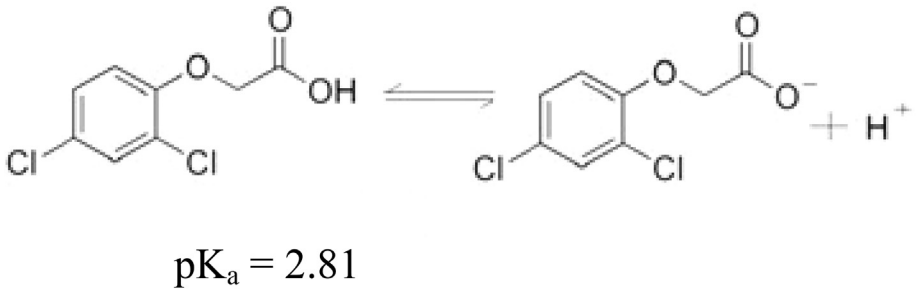

Fig. 1. Protonated and deprotonated species of 2,4-D.

acidic nature of 2,4-D. Samples were taken at regular intervals from 0 to 10 min of irradiation. Experimental data were analyzed using Eq. (2) to calculate the apparent rate constants. A control experiment was conducted in the dark with 2.5 mol H_2O_2 per mol of 2,4-D for a period of 30 days, and no significant degradation of 2,4-D was observed.

The effects of initial 2,4-D concentration (10–100 mg L^{-1} or 0.045–0.45 mM), pH (4–8), alkalinity (0–5 mM as HCO_3^-), nitrate (0–1 mM), and ionic strength (0–1000 mg L^{-1} or 0–17 mM, as NaCl) on 2,4-D transformation were studied for the UV-H_2O_2 AOP. In addition, 2,4-D degradation experiments were conducted in a real surface water. In all cases, the initial 2,4-D and H_2O_2 concentrations were 100 mg L^{-1} (0.45 mM) and 38 mg L^{-1} (1.125 mM) H_2O_2, unless otherwise stated. The pH of experimental solutions was adjusted using 10 mM phosphate buffer. Surface water samples were collected from Neem Lake (Shibpur, India) and passed through 2.5-μm filters (Whatman). The filtrate had the following composition: 236 mg L^{-1} as $CaCO_3$ of alkalinity; 2.5 mg L^{-1} of nitrate; pH 7.8; 40 mg L^{-1} of five-day biochemical oxygen demand (BOD_5); 150 mg L^{-1} of chemical oxygen demand (COD); 896 mg L^{-1} of total solids; and, 360 mg L^{-1} dissolved solids.

The biodegradability of 2,4-D transformation products was examined for direct photolysis at 253.7 nm and UV-H_2O_2 treatment. In this regard, the ratio of BOD_5 to COD was used to describe changes in biodegradability [30]. The dilution method, followed by DO measurement by the Winkler Method, was adopted to calculate BOD_5 [31]. The standard closed reflux titrimetric method with potassium dichromate was used to determine COD levels [31].

All data are reported as the mean ± standard deviation (n = 3), unless otherwise stated. Analysis of variance (ANOVA) calculations for experimental data were carried out in Microsoft Excel. Significant differences were defined using 95% confidence intervals ($p < 0.05$).

3. Results and discussion

3.1. The pH dependence of 2,4-D molar absorption coefficients

The absorbance of 2,4-D solutions buffered at pH 1–8 was measured by UV–vis spectrophotometry as discussed in section 2.3. The Beer-Lambert law was used to determine the corresponding apparent molar absorption coefficients at 220–300 nm. A heatmap showing the relationship between the apparent molar absorption coefficient of 2,4-D, wavelength, and pH is shown in Fig. 2. The apparent molar absorption coefficient of 2,4-D was lower at strongly acidic pH, indicating that the protonated form of 2,4-D absorbed less light than the deprotonated species, which dominates at pH > 2.81 (*i.e.*, $pK_{a,2,4\text{-D}}$). The molar absorption coefficient above pH 5 was effectively constant as 2,4-D does not undergo further deprotonation. Two absorbance peaks were identified for 2,4-D at 230 nm and 283 nm. The variation in 2,4-D molar

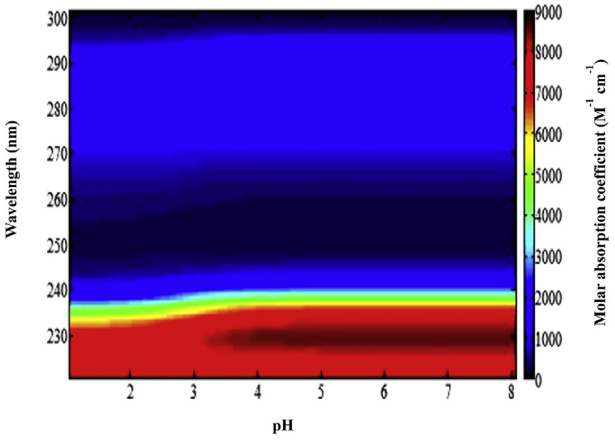

Fig. 2. Map of apparent molar absorptivity ($M^{-1}cm^{-1}$) for 2,4-D as a function of pH (1–8) and wavelength (220–300 nm).

absorption coefficients at 230 nm and 283 nm with solution pH is shown in Fig. 3. Note that the molar absorption coefficient of 2,4-D is low at 253.7 nm (*i.e.*, 150-270 M^{-1} cm^{-1}), suggesting that direct photolysis with low-pressure lamps may not be an effective treatment strategy.

3.2. Direct photolysis of 2,4-D at 253.7 nm

The degradation of 2,4-D was studied under UV irradiation at 253.7 nm for an initial 2,4-D concentration of 100 mg L^{-1} (0.45 mM) and pH 4.0 (±0.1). From the molar absorption

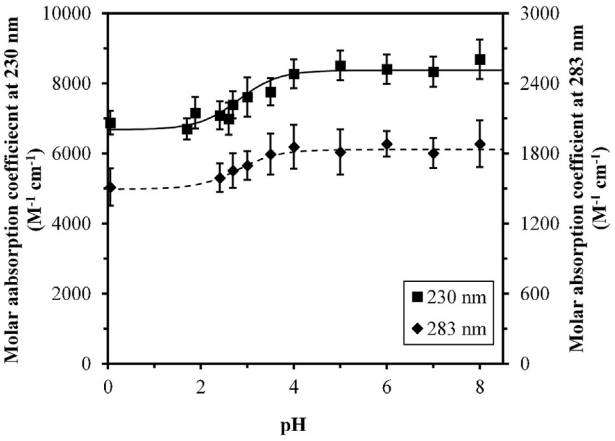

Fig. 3. The apparent molar absorptivity of 2,4-D at 230 nm and 283 nm modelled using Eq. (1). Symbols are experimentally-measured data and curves are the best model fits.

coefficients in Fig. 3, the transformation kinetics at pH 4.0 (±0.1) are expected to be similar to those at pH 5–8 with all other conditions being equal. Approximately 66% degradation was observed for 3 h (20 J cm^{-2}) of treatment (Fig. 4). Over the irradiation period, the solution color changed from clear to yellow due to the formation of chromophoric 2,4-D transformation products, including 2,4-dichlorophenol (DCP) and chlorohydroquinone (CHQ), which exhibit a yellow color in solution [32–34]. The corresponding transformation mechanisms, namely loss of the acetic acid group and hydroxylation of the aromatic ring, align with previously reported UV reactions [35]. 2,4-D degradation followed pseudo-first-order reaction kinetics and Eq. (2) was applied to calculate the apparent fluence-based rate constant for pH 4.0 (±0.1), namely 5.77 (±0.66) × 10^{-5} cm^2 mJ^{-1}. An apparent fluence-based rate constant for 2,4-D of 1.3 × 10^{-4} cm^2 mJ^{-1} was previously reported in a medium-pressure UV reactor system emitting at 290–320 nm [23]; this result likely stemmed from the increased absorbance at 280–300 nm.

The apparent fluence-based, pseudo-first-order rate constants were used to calculate apparent quantum yields according to Eq. (3) [27].

$$\Phi_{253.7,app} = \frac{k'_{p,app}\, U_{253.7}}{\varepsilon_{253.7,app} \ln 10} \quad (3)$$

In Eq. (3), $\Phi_{253.7,app}$ is the apparent quantum yield at 253.7 nm (mol Einstein^{-1}), $k'_{p,app}$ is the experimentally-determined, apparent fluence-based pseudo-first-order rate constant (cm^2 mJ^{-1}), $\varepsilon_{253.7,app}$ is the apparent molar absorption coefficient at 253.7 nm (M^{-1} cm^{-1}), and $U_{253.7}$ is the molar photon energy at 253.7 nm (*i.e.*, 4.72 × 10^5 J E^{-1}). The quantum yield describes the phototransformation efficiency and is defined as the moles of a compound that are transformed per mole of photons absorbed [36]. The quantum yield for degradation of 2,4-D was found to be 7.04 (±0.21) × 10^{-2} mol E^{-1}, indicating a photo-transformation efficiency of ~7%. For medium-pressure systems, the quantum yield was reported to be 3.6 (±0.3) × 10^{-3} mol E^{-1} [23]. These results confirm that the reaction is more efficient at 253.7 nm, but the lower absorbance of light at 253.7 nm limits the overall fluence-based reaction kinetics.

3.3. UV-H_2O_2 degradation of 2,4-D

Apparent fluence-based, pseudo-first-order rate constants were calculated using the kinetics data collected from experiments with different H_2O_2 doses. The average 2,4-D degradation increased as the ratio of H_2O_2 to 2,4-D increased from 0 to 2.5 mol/mol but decreased for higher H_2O_2 doses (Fig. 5); however, the rate constants were not significantly different for the 0.5–5.0 mol H_2O_2 per mol 2,4-D conditions. The 2,4-D transformation efficiency significantly decreased at higher H_2O_2 doses due to H_2O_2 scavenging of hydroxyl radicals, as observed in previous studies [26,37]. These results suggest that the hydroxyl radical yield from the UV-H_2O_2 process was the driving force behind enhanced 2,4-D transformation.

Degradation of 2,4-D in the UV-H_2O_2 process was found to be 100 times faster than UV irradiation when 2.5 mol H_2O_2 per mol 2,4-D was employed. Fig. 6 shows the degradation of 2,4-D at a peroxide dose of 2.5 mol of H_2O_2 per mol 2,4-D. Approximately 97% degradation was observed within 6 min, corresponding to a fluence of 678 mJ cm^{-2}. The fluence required for the same extent of 2,4-D degradation by direct photolysis was extrapolated using $k'_{p,app}$ from Fig. 4 to be 61 J cm^{-2}. To contextualize the magnitude of these required treatments, consider that UV disinfection of wastewater typically employs a fluence of 40–190 mJ cm^{-2} [25,38]. Consequently, 50–70% 2,4-D transformation could be achieved at disinfection-level UV doses with suitable H_2O_2 addition, while only 2% could be attained without H_2O_2. Importantly, previous efforts have demonstrated that the cost of UV-H_2O_2 photo-oxidation of the herbicide ametryn was lower than UV irradiation alone due to the lower fluence requirement [8].

3.3.1. Effect of initial 2,4-D concentration

Degradation of 10–100 mg L^{-1} 2,4-D was studied with H_2O_2 doses of 3.06–30.6 mg L^{-1} (0.09–0.9 mM) H_2O_2 at pH 4.0 (±0.1). At higher concentrations, 2,4-D degradation was slower. For example, the 2,4-D degradation percentages for a fluence of 113 mJ cm^{-2} were 85, 70, 60, and 49 for initial concentrations of 10, 50, 75, and

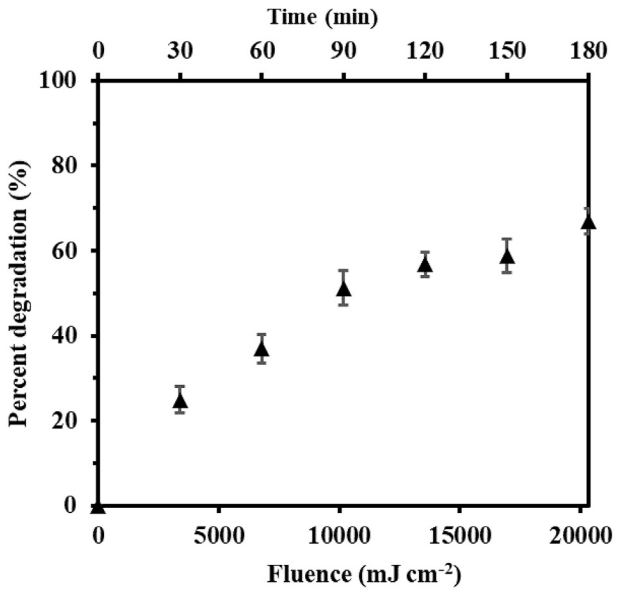

Fig. 4. Degradation of 100 mg L^{-1} (0.45 mM) of 2,4-D by direct UV irradiation at 253.7 nm at pH 4.0 (±0.1) as a function of time and fluence.

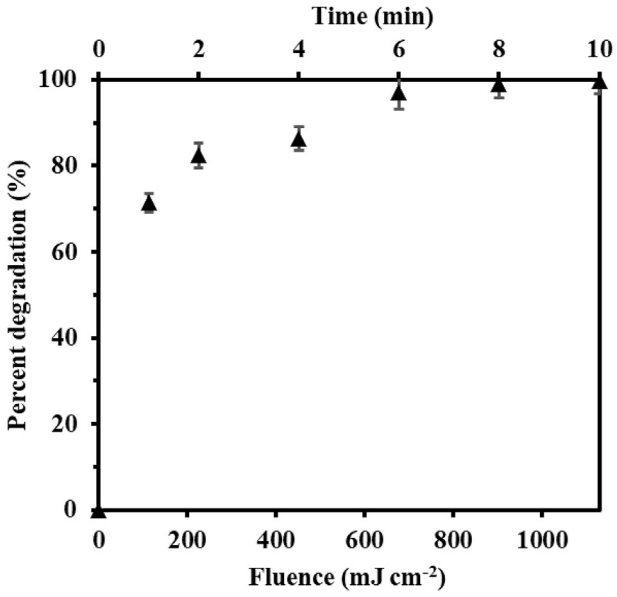

Fig. 5. Photodegradation of 100 mg L^{-1} (0.45 mM) of 2,4-D with 1.125 mM H_2O_2 dose at pH 4.0 (±0.1) as a function of time and fluence.

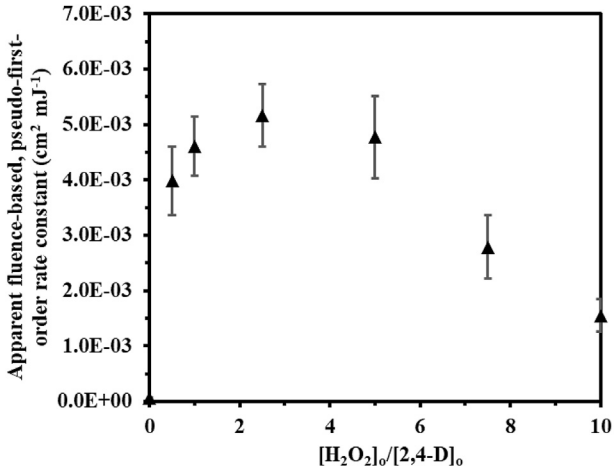

Fig. 6. Effect of H_2O_2 dose (0–10 mol H_2O_2 per mol 2,4-D; with an initial 2,4-D concentration of 100 mg L^{-1} (0.45 mM) on the apparent fluence-based, pseudo-first order rate constant for 2,4-D degradation at pH 4.0 (±0.1).

100 mg L^{-1} respectively. The apparent fluence-based, pseudo-first-order rate constants for different initial 2,4-D concentrations are shown in Fig. 7. Similar behavior has been observed for UV/H_2O_2 degradation of compounds like microcystin–LR and diethanolamine [39,40]. Since the molar absorption coefficients of 2,4-D (169.6 at pH 4) and H_2O_2 (19.6 $M^{-1}cm^{-1}$) at 257.7 nm are high it is expected that higher 2,4-D concentration will not affect hydroxyl generation much. However, when 2,4-D concentration is high, the concentration of H_2O_2 is also high which may scavenge the hydroxyl radical. Thus, the rate constant decreased with increasing 2,4-D concentration.

3.3.2. Effect of pH

For the optimal 2.5 mol H_2O_2 per mol 2,4-D conditions, the solution pH was varied in the 4–8 range using 10 mM phosphate buffer to determine pH effects on transformation kinetics in the UV-H_2O_2 system. The treatment efficiency dropped from 97% at pH 4–85% at pH 8 for a fluence of 678 mJ cm^{-2}. In general, the apparent fluence-based, pseudo-first-order rate constant decreased with solution pH, as indicated in Fig. 8. The steady state hydroxyl radical concentrations at pH 4 and 8 were calculated to be 11.66 $(\pm 1.27) \times 10^{-11}$ M and 6.96 $(\pm 0.83) \times 10^{-11}$ M, respectively, presumably due to differences in the dissolved carbonate system. The lower hydroxyl radical exposure resulted in the slower 2,4-D degradation observed in Fig. 8. A similar decrease in hydroxyl radical concentrations were reported at higher pH in the UV-H_2O_2 process [41].

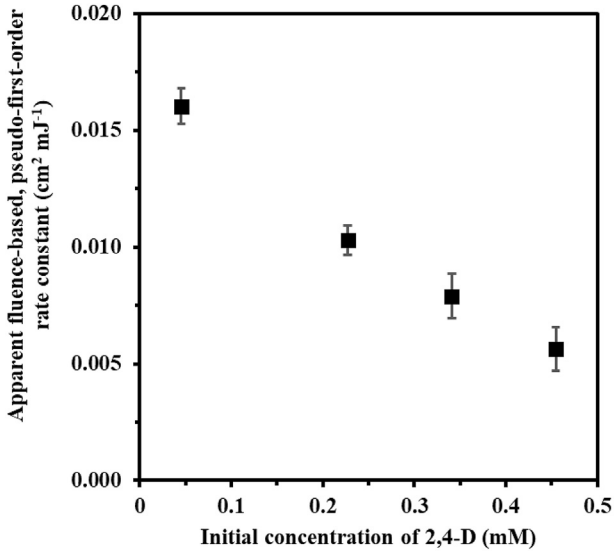

Fig. 7. Effect of initial concentration on 2,4-D degradation with 0.90 mM H_2O_2 dose at pH 4.0 (±0.1).

3.3.3. Effect of alkalinity

Bicarbonate, nitrate, ionic strength (as NaCl) concentrations influence the efficiency of AOPs to transform micropollutants in wastewater [42]. The effects of alkalinity on 2,4-D transformation were investigated by adding 0–5 mM HCO_3^- to solutions containing 100 mg L^{-1} (0.45 mM) of 2,4-D with 38 mg L^{-1} (1.125 mM) H_2O_2 at pH 7.5 (±0.1). The second-order rate constants for reaction of hydroxyl radicals with bicarbonate and 2,4-D are 8.5×10^6 M^{-1} s^{-1} [43] and 5×10^9 $M^{-1}s^{-1}$ [44], respectively. Even though 2,4-D reacts with HO• faster than bicarbonate, the apparent fluence-based rate constant for 2,4-D degradation in the UV-H_2O_2 process decreased slightly with increasing bicarbonate concentration (Fig. 9). The fraction of hydroxyl radicals that reacted with bicarbonate compared to other species was determined with Eq. (4) (adapted from Adak et al. [27]).

$$f_{HO^\bullet,HCO_3^-} = \frac{k''_{HO^\bullet,HCO_3^-}\left[HCO_3^-\right]}{k''_{HO^\bullet,2,4\text{-D}}[2,4\text{-D}] + k''_{HO^\bullet,HCO_3^-}\left[HCO_3^-\right] + \sum_{i=1}^{n} k''_{HO^\bullet,S_i}[S_i]} \quad (4)$$

In Eq. (4), $f_{HO^\bullet,HCO_3^-}$ is the fraction of HO• scavenged by HCO_3^- and $k''_{HO^\bullet,i}$ is the second-order rate constant for HO• reaction with HCO_3^-, 2,4-D, or other species (S).

The fraction of hydroxyl radicals consumed by bicarbonate was calculated to be 3.7×10^{-3}, 9.2×10^{-3}, and 18.2×10^{-3} for bicarbonate concentrations of 1.0, 2.5, and 5.0 mM, respectively. Hydroxyl radical scavenging by bicarbonate, therefore, resulted in a lower fraction of hydroxyl radicals available for reaction with 2,4-D. Similar expressions can be written to define $f_{HO^\bullet,H_2O_2}$, $f_{HO^\bullet,P(V)}$, and $f_{HO^\bullet,2,4\text{-D}}$ to determine the fraction of hydroxyl radicals that were scavenged by H_2O_2 and phosphate buffer and reacted with 2,4-D. In this case, the hydroxyl radical demands of H_2O_2 and the P(V) buffer system were about 1.3% and 0.03%, respectively. The fraction of

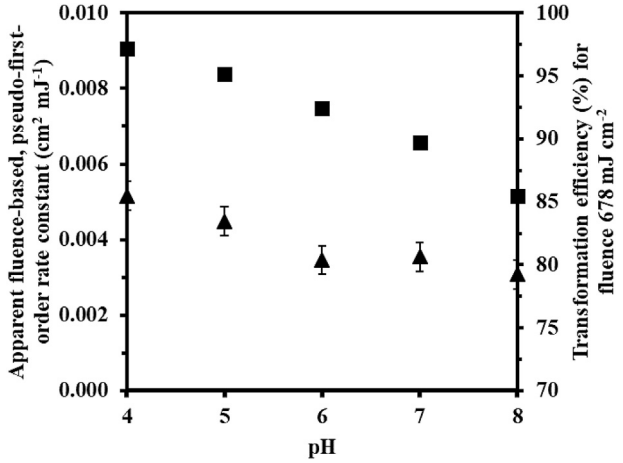

Fig. 8. Effect of solution pH on the apparent fluence-based, pseudo-first-order rate constant for 2,4-D degradation for UV-H_2O_2 treatment with 1.125 mM H_2O_2 dose and the corresponding 2,4-D transformation efficiency for a fluence of 678 mJ cm^{-2}.

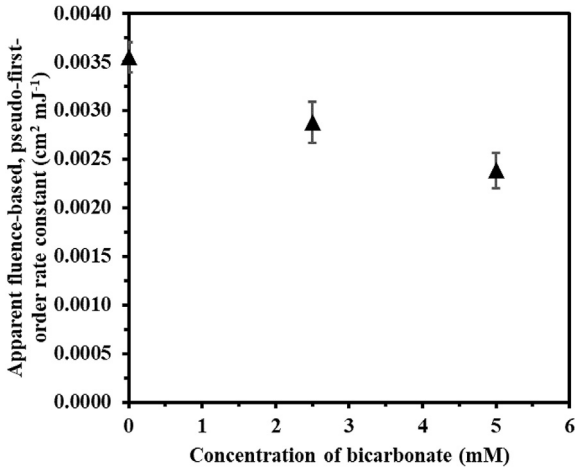

Fig. 9. Effect of alkalinity (expressed as HCO_3^- concentration) on 2,4-D degradation kinetics for $[2,4\text{-D}]_o = 100\ mg\ L^{-1}$ (0.45 mM), H_2O_2 dose = 1.125 mM, and pH = 7.5 (±0.1).

hydroxyl radicals that reacted with 2,4-D for the 1.0, 2.5, and 5.0 mM HCO_3^- conditions was 0.98, 0.97, and 0.96, respectively. These findings indicate that alkalinity differences in 2,4-D contaminated water moderately impact the observed reaction kinetics in UV-H_2O_2 systems for the investigated solution chemistry.

3.4. Effect of nitrate concentration

Since herbicide-contaminated water resources are also impacted by fertilizer application, the effect of 0–1 mM nitrate on 2,4-D photodegradation was studied. The experimental conditions involved 38 mg L^{-1} (1.125 mM) H_2O_2 dose with 100 mg L^{-1} of 2,4-D (0.45 mM) at pH 4.0 (±0.1). Apparent fluence-based, pseudo-first-order rate constants were calculated (Fig. 10). The observed rate constant decreased for increasing nitrate concentrations due to HO• scavenging ($k''_{HO^\bullet,NO_3^-} = 9.7 \times 10^9\ M^{-1}\ s^{-1}$ [43]). Using a modified version of Eq. (4), the fraction of HO• reacting with NO_3^- was 0.67 and 0.80 for nitrate concentrations of 0.50 and 1.0 mM, respectively. Hydroxyl radical scavenging by nitrate, therefore, resulted in a lower fraction of hydroxyl radicals reacting with 2,4-D (*i.e.*, $f_{HO\bullet,2,4\text{-}D} = 0.32$ and 0.19 for the 0.5 and 1.0 mM NO_3^- concentrations, respectively). The hydroxyl radical demand of hydrogen peroxide for these experiments was approximately 1.0%. These inhibitory effects, which have also been reported for 1,2-dibromo-3-chloropropane [26], may be a deterrent to the use of the UV-H_2O_2 process in groundwater systems with high nitrate concentrations.

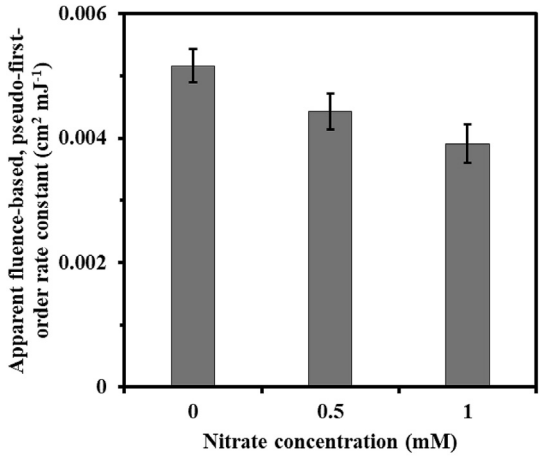

Fig. 10. Nitrate (0–1 mM) effects on 100 mg L^{-1} (0.45 mM) of 2,4-D degradation in the UV-H_2O_2 process with 1.125 mM H_2O_2 dose and pH 4.0 (±0.1).

3.5. Effect of ionic strength

2,4-D degradation by the UV-H_2O_2 process was examined at various ionic strengths in the range of 0–17 mM (as NaCl). The initial 2,4-D concentration was 0.45 mM with H_2O_2 dose of 30.6 mg L^{-1} (0.9 mM) and pH 4.0 (±0.1). The degradation kinetics of 2,4-D were unaffected by the increase in ionic strength (see Fig. S2 in the supplementary information). Similar behavior has been observed for advanced oxidation of flumequine [42].

3.6. Effect of surface water matrix

The applicability of the UV-H_2O_2 process for treatment of agriculturally-impacted water was studied using surface water samples spiked with 100 mg L^{-1} (0.45 mM) 2,4-D. Initially, the solution had 40.4 mg L^{-1} of BOD_5 and 149.8 mg L^{-1} of COD. Other water quality conditions were mentioned in section 2.3. The molar ratio of H_2O_2 to 2,4-D was 2.5 and the pH was 7.5 (±0.1). The fluence-based rate constant for 2,4-D transformation was 2.5 (±0.3) × 10^{-3} $cm^2\ mJ^{-1}$ (Fig. 11). This rate constant was similar to that determined above (Fig. 9) for a bicarbonate concentration of 2.5 mM, which is similar to the 236 mg L^{-1} as $CaCO_3$ alkalinity of the surface water; however, the apparent 2,4-D rate constant in the surface water matrix was ~50% of that obtained for distilled water under similar conditions. The slower reaction kinetics are likely due to scavenging effects stemming from the carbonate system and dissolved organic matter [45,46].

3.7. Biodegradability enhancement after UV-H_2O_2 treatment

The BOD_5/COD ratio for 100 mg L^{-1} (0.45 mM) of 2,4-D was 0.08 (±0.02), indicating that 2,4-D is not biodegradable [47]. Due to the high operating costs of AOPs, application of partial oxidation followed by biological polishing is being pursued for recalcitrant

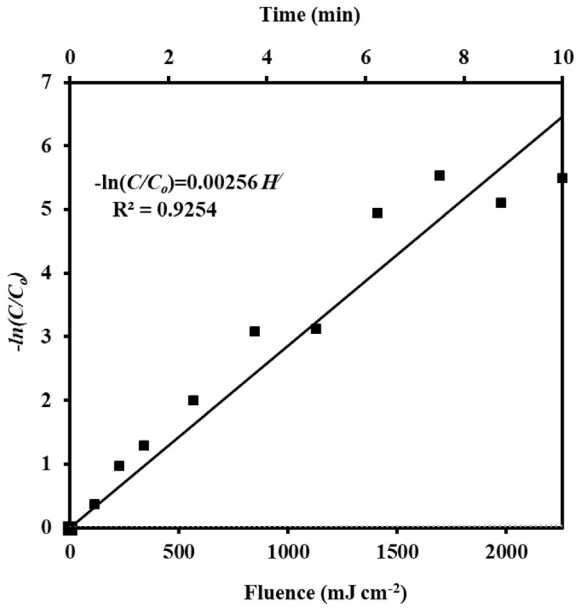

Fig. 11. Apparent pseudo-first-order reaction kinetics for 100 mg L^{-1} (0.45 mM) of 2,4-D degradation in surface water with 1.125 mM H_2O_2 dose and pH 7.5 (±0.1).

pollutants like 2,4-D [48]. Degradation of 2,4-D using the UV-H_2O_2 process results in formation of a number of transformation products: 2,4-dichlorophenol; chlorohydroquinone; organic acids, such as acetate, glycolate, formate, malonate, oxalate, and fumarate; and, chloride [32–34]. For these reasons, the biodegradability of UV-H_2O_2 treated wastewater containing 2,4-D was measured using BOD_5. In particular, 100 mg L^{-1} (0.45 mM) 2,4-D solutions were treated with UV irradiation at fluences of 6.7, 13.3, and 20 J cm^{-2} and UV-H_2O_2 advanced oxidation with fluences of 282, 565, 848, and 1130 mJ cm^{-2} at H_2O_2 dose of 1.125 mM. Residual H_2O_2 in the treated samples was quenched by catalase before measurement of COD and BOD_5. The COD and BOD_5 of catalase was accounted for using controls containing only catalase.

For UV degradation, the BOD_5/COD ratio increased from 0.08 to 0.28 over 3 h (or 20 J cm^{-2} fluence) of irradiation, as shown in Fig. 12. The increase in BOD_5/COD indicates that the biodegradability of 2,4-D treated effluent was enhanced by direct photolysis. On the other hand, the BOD_5/COD ratio increased from 0.10 to 0.63 for UV-H_2O_2 treatment with a fluence of 1130 mJ cm^{-2} (Fig. 12). The BOD_5 increased from 25 to 100 mg L^{-1} in 5 min and decreased with further treatment. These results demonstrate that transformation products were more biodegradable than the 2,4-D parent compound. Since the BOD_5/COD ratio in the UV-H_2O_2 treated solution was 0.63, the effluent can be effectively treated by biological processes to remove potential concerns associated with transformation products [47].

4. Conclusion

Disinfection-level UV treatment at 253.7 nm transforms a nominal fraction of 2,4-D in water and highlights the need for higher fluence or advanced processes to attain significant transformation efficiencies. For the UV-H_2O_2 process, more than 97% transformation of 2,4-D was achieved with a fluence of 678 mJ cm^{-2} and 2.5 mol H_2O_2 per mol 2,4-D. The apparent rate constants for UV irradiation at 253.7 nm (*i.e.*, 5.77 $(\pm 0.66) \times 10^{-5}$ cm^2 mJ^{-1}) and UV-H_2O_2 treatment (*i.e.*, 5.16 $(\pm 0.56) \times 10^{-3}$ cm^2 mJ^{-1} for 2.5 mol H_2O_2 per mol of 2,4-D) determined here are applicable to other systems; however, initial 2,4-D concentration, pH, alkalinity, and nitrate concentration affect the extent of 2,4-D transformation. The apparent rate constant for 2,4-D degradation decreased at higher 2,4-D concentrations. The apparent fluence-based, pseudo-first-order rate constant decreased by a factor of 1.7 when pH was increased from 4 to 8, and a similar effect was observed for nitrate concentrations up to 1 mM. The effects of alkalinity up to 5 mM of HCO_3^- and ionic strength up to 17 mM (as NaCl) demonstrated minor impacts on 2,4-D degradation kinetics. In aggregate, these results indicate the importance of water/wastewater quality on treatment metrics. Overall, the UV-H_2O_2 process provided quick and efficient transformation of 2,4-D to biodegradable products that can be treated via conventional biological systems. Thus, the UV-H_2O_2 process is proposed for treatment of concentrated herbicide solutions generated in agricultural systems.

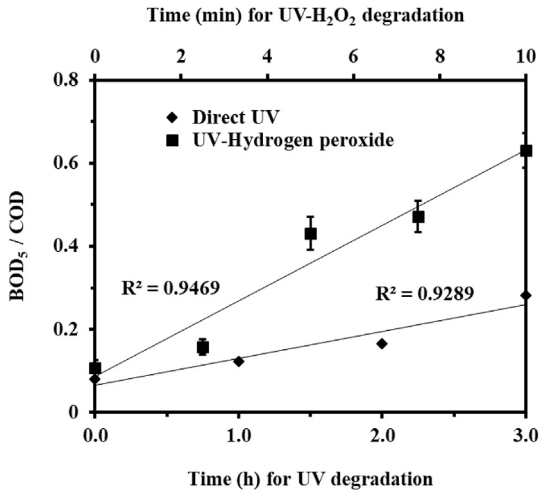

Fig. 12. Effect of direct photolysis at 253.7 nm and UV-H_2O_2 treatment on biodegradability index (BOD_5/COD ratio) of a solution that initially contained 100 mg L^{-1} (0.45 mM) of 2,4-D.

Acknowledgement

The authors acknowledge the Technical Education Quality Improvement Programme - III for providing High Performance Liquid Chromatography in the Environmental Engineering Laboratory which was used to detect 2,4-D.

Appendix A. Supplementary data

Supplementary data to this article can be found online at https://doi.org/10.1016/j.emcon.2019.02.004.

References

[1] S. Sanchis, A.M. Polo, M. Tobajas, J.J. Rodriguez, A.F. Mohedano, Degradation of chlorophenoxy herbicides by coupled Fenton and biological oxidation, Chemosphere 93 (2013) 115–122.
[2] K. Ikehata, M. Gamal El-Din, Degradation of aqueous pharmaceuticals by ozonation and advanced oxidation processes: a review, Ozone Sci. Eng. 28 (2006) 353–414.
[3] S.Z. Lari, N.A. Khan, K.N. Gandhi, T.S. Meshram, N.P. Thacker, Comparison of pesticide residues in surface water and ground water of agriculture intensive areas, J. Environ. Heal. Sci. Eng. 12 (11) (2014) 1–7.
[4] P.K. Mutiyar, A.K. Mittal, Status of organochlorine pesticides in Ganga river basin: anthropogenic or glacial? Drink. Water Eng. Sci. 6 (6) (2013) 69–80.
[5] I.C. Yadav, N.L. Devi, J.H. Syed, Z. Cheng, J. Li, G. Zhang, Current status of persistent organic pesticides residues in air, water, and soil, and their possible effect on neighboring countries: a comprehensive review of India, Sci. Total Environ. 511 (2015) 123–137.
[6] D.P. Mukherjee, K. Bhupander, K. Sanjay, M. Meenu, G. Richa, P. Dev, Occurrence and distribution of pesticide residues in selected seasonal vegetables from West Bengal, Arch. Appl. Sci. Res. 3 (2011) 85–93.
[7] K. Ikehata, M. Gamal El-Din, Aqueous pesticide degradation by ozonation and ozone-based advanced oxidation processes: a review (Part I), Ozone Sci. Eng. 27 (2005) 83–114.
[8] W. Chu, N. Gao, C. Li, J. Cui, Photochemical degradation of typical halogenated herbicide 2,4-D in drinking water with UV/H_2O_2/micro-aeration, Sci. China Ser. B Chem. 52 (2009) 2351–2357.
[9] S. Koner, A. Pal, A. Adak, Adsorption of 2,4-D herbicide from water environment on modified silica gel factory waste, Water Environ. Res. 85 (2013) 2147–2156.
[10] V.K. Gupta, B. Gupta, A. Rastogi, S. Agarwal, A. Nayak, Pesticides removal from waste water by activated carbon prepared from waste rubber tire, Water Res. 45 (2011) 4047–4055.
[11] J.M. Salman, Optimization of preparation conditions for activated carbon from palm oil fronds using response surface methodology on removal of pesticides from aqueous solution, U. A. R. J. Chem. 7 (2014) 101–108.
[12] S. Nethaji, A. Sivasamy, Graphene oxide coated with porous iron oxide ribbons for 2, 4-Dichlorophenoxyacetic acid (2,4-D) removal, Ecotoxicol. Environ. Saf. 138 (2017) 292–297.
[13] L.C. Lu, C.I. Wang, W.F. Sye, Applications of chitosan beads and porous crab shell powder for the removal of 17 organochlorine pesticides (OCPs) in water solution, Carbohydr. Polym. 83 (2011) 1984–1989.
[14] R. Shiralipour, B. Zargar, H. Parham, Temephos removal from water samples by silver modified zero-valent iron nanoparticles, Jundishapur J. Heal. Sci. 7 (2015) 1–8.
[15] V.K. Gupta, I. Ali, V.K. Suhas Saini, Adsorption of 2,4-D and carbofuran pesticides using fertilizer and steel industry wastes, J. Colloid Interface Sci. 299 (2006) 556–563.
[16] T.P.A. Shabeer, A. Saha, V.T. Gajbhiye, S. Gupta, K.M. Manjaiah, E. Varghese, Simultaneous removal of multiple pesticides from water: effect of organically modified clays as coagulant aid and adsorbent in coagulation–flocculation process, Environ. Technol. 35 (2014) 2619–2627.

[17] A. Bhattacharya, P. Ray, H. Brahmbhatt, K.N. Vyas, S.V. Joshi, C.V. Devmurari, J.J. Trivedi, Pesticides removal performance by low-pressure reverse osmosis membranes, J. Appl. Polym. Sci. 102 (2006) 3575–3579.
[18] J.O. Ka, W.E. Holben, J.M. Tiedje, Genetic and phenotypic diversity of 2,4-dichlorophenoxyacetic acid (2,4-D)-degrading bacteria isolated from 2,4-D-treated field soils, Appl. Environ. Microbiol. 60 (1994) 1106–1115.
[19] J.M. Fontmorin, S. Huguet, F. Fourence, F. Geneste, D. Floner, A. Amrane, Electrochemical oxidation of 2,4-dichlorophenoxyacetic acid: analysis of by-products and improvement of the biodegradability, Chem. Eng. J. 195 (2012) 208–217.
[20] D. Şolpan, M. Torun, The removal of chlorinated organic herbicide in water by gamma-irradiation, J. Radioanal. Nucl. Chem. 293 (2012) 21–38.
[21] K.H.H. Aziz, H. Miessner, S. Mueller, A. Mahyar, D. Kalass, D. Moeller, I. Khorshid, M.A.M. Rashid, Comparative study on 2,4-dichlorophenoxyacetic acid and 2,4-dichlorophenol removal from aqueous solutions via ozonation, photocatalysis and non-thermal plasma using a planar falling film reactor, J. Hazard Mater. 343 (2018) 107–111.
[22] J.M. Fontmorin, F. Fourcade, F. Geneste, I. Soutrel, D. Floner, A. Amrane, Direct electrochemical oxidation of a pesticide, 2,4-dichlorophenoxyacetic acid, at the surface of a graphite felt electrode: biodegradability improvement, Compt. Rendus Chem. 18 (2014) 32–38.
[23] Z. Shu, J.R. Bolton, M. Belosevic, M. Gamal El Din, Photodegradation of emerging micropollutants using the medium-pressure UV/H_2O_2 advanced oxidation process, Water Res. 47 (2013) 2881–2889.
[24] F.J. Beltran, G. Ovejero, B. Acedo, Oxidation of atrazine in water by ultraviolet radiation combined with hydrogen peroxide, Water Res. 27 (1993) 1013–1021.
[25] C. Baeza, D.R.U. Knappe, Transformation kinetics of biochemically active compounds in low-pressure UV photolysis and UV/H_2O_2 advanced oxidation processes, Water Res. 45 (2011) 4531–4543.
[26] W.H. Glaze, Y. Lay, J.W. Kang, Advanced oxidation processes. kinetic model for the oxidation of 1,2-dibromo-3-chloropropane in water by the combination of hydrogen peroxide and UV radiation, Ind. Eng. Chem. Res. 37 (1995) 2314–2323.
[27] A. Adak, K.P. Mangalgiri, Lee, L. Blaney, UV irradiation and UV-H_2O_2 advanced oxidation of the roxarsone and nitarsone organoarsenicals, Water Res. 70 (2015) 74–85.
[28] A. Lopez, A. Bozzi, G. Mascolo, J. Kiwi, Kinetic investigation on UV and UV/H_2O_2 degradations of pharmaceutical intermediates in aqueous solution, J. Photochem. Photobiol. Chem. 156 (2003) 121–126.
[29] C.G. Hatchard, C.A. Parker, A new sensitive chemical actinometer II. potassium ferrioxalate as a standard chemical actinometer, Proc. Roy. Soc. Lond. 235 (1203) (1956) 518–536.
[30] E. Chamarro, A. Marco, S. Esplugas, Use of Fenton reagent to improve organic chemical biodegradability, Water Res. 35 (2001) 1047–1051.
[31] APHA, AWWA, WEF, Standard Methods for Examination of Water and Wastewater, twentith ed., 1998. Washington DC.
[32] O.M. Alfano, R.J. Brandi, A.E. Cassano, Degradation kinetics of 2,4-D in water employing hydrogen peroxide and UV radiation, Chem. Eng. J. 82 (2001) 209–218.
[33] C.Y. Kwan, W. Chu, Photodegradation of 2,4- dichlorophenoxyacetic acid in various iron-mediated oxidation systems, Water Res. 37 (2003) 4405–4412.
[34] K. Ikehata, M.G. El-din, Aqueous pesticide degradation by hydrogen peroxide/ultraviolet irradiation and Fenton-type advanced oxidation processes : a review, J. Environ. Eng. Sci. 135 (2006) 81–135.
[35] E. Brillas, J.C. Calpe, J. Casado, Mineralization of 2,4-D by advanced electrochemical oxidation processes, Water Res. 34 (2000) 2253–2262.
[36] J.R. Bolton, M.I. Stefan, Fundamental photochemical approach to the concepts of fluence (UV dose) and electrical energy efficiency in photochemical degradation reactions, Res. Chem. Intermed. 28 (2002) 857–870.
[37] R.R. Giri, H. Ozaki, Y. Takayanagi, S. Taniguchi, R. Takanami, Efficacy of ultraviolet radiation and hydrogen peroxide oxidation to eliminate large number of pharmaceutical compounds in mixed solution, Int. J. Environ. Sci. Technol. 8 (2010) 19–30.
[38] O.S. Keen, N.G. Love, K.G. Linden, The role of effluent nitrate in trace organic chemical oxidation during UV disinfection, Water Res. 46 (2012) 5224–5234.
[39] X. He, M. Pelaez, J.A. Westrick, et al., Efficient removal of microcystin-LR by UV-C/H_2O_2 in synthetic and natural water samples, Water Res. 46 (5) (2011) 1501–1510.
[40] N. Madihah, B. Yaser, F. Chemat, et al., Degradation of aqueous diethanolamine (DEA) solutions using UV/H_2O_2 process, Chem. Eng. Trans. 43 (2015) 1–6.
[41] E.J. Rosenfeldt, K.G. Linden, S. Canonica, U. Von Gunten, Comparison of the efficiency of ˙OH radical formation during ozonation and the advanced oxidation processes, Water Res. 40 (2006) 3695–3704.
[42] F. Mingbao, Q. Ruijuan, X. Zhang, et al., Degradation of flumequine in aqueous solution by persulfate activated with common methods and polyhydroquinone-coated magnetite/multi-walled carbon nanotubes catalysts, Water Res. 85 (2015) 1–10.
[43] G.V. Buxton, C.L. Greenstock, W.P. Helman, A.B. Ross, Critical review of rate constants for reactions of hydrated electrons, hydrogen atoms and hydroxyl radicals in aqueous solution, J. Phys. Chem. Ref. Data 17 (1988) 513–886.
[44] M. Mariani, R. Romero, A. Cassano, C. Zalazar, Degradation of mixture of glyphosate and 2,4-D in water solution employing the UV/H_2O_2 process including toxicity ealuation, in: M.I. Litter, R.J. Candal, J.M. Meichtry (Eds.), Advanced Oxidation Technologies: Sustainable Solutions for Environmental Treatments, CRC Press, Boca Raton, 2014, pp. 99–114.
[45] S.R. Cater, M.I. Stefan, J.R. Bolton, A. Safarzadeh-Amiri, UV/H_2O_2 treatment of methyl tert-butyl ether in contaminated waters, Environ. Sci. Technol. 34 (2000) 659–662.
[46] G.S. Wang, C.H. Liao, H.W. Chen, H.C. Yang, Characteristics of natural organic matter degradation in water by UV/H_2O_2 treatment, Environ. Technol. 27 (2006) 277–287.
[47] S.K. Garg, R. Garg, Quality and characteristics of sewage, in: Sewage Disposal and Air Pollution Engineering, 24th Ed., Khanna Publishers, New Delhi, 2012, pp. 147–187.
[48] W.K. Lafi, Z. Al-Qodah, Combined advanced oxidation and biological treatment processes for the removal of pesticides from aqueous solutions, J. Hazard Mater. 137 (2006) 489–497.